

**SYNTHESIS, CHARACTERIZATION,  
MESOMORPHIC PROPERTIES AND  
MOLECULAR MODEL STUDY OF NON-LINEAR  
DISULPHIDE CENTRED LIQUID CRYSTAL  
OLIGOMERS**

**YAP PUI WING**

**UNIVERSITI SAINS MALAYSIA**

**2025**

**SYNTHESIS, CHARACTERIZATION,  
MESOMORPHIC PROPERTIES AND  
MOLECULAR MODEL STUDY OF NON-LINEAR  
DISULPHIDE CENTRED LIQUID CRYSTAL  
OLIGOMERS**

by

**YAP PUI WING**

**Thesis submitted in fulfilment of the requirements  
for the degree of  
Doctor of Philosophy**

**February 2025**

## ACKNOWLEDGEMENT

First of all, I would like to express thousands of my deepest gratitude to my former main supervisor, Professor ChM. Dr. Yeap Guan Yeow for his passion in guiding and consistent supporting throughout my candidature period. It was indeed a pleasure and great experience to pursue my PhD degree under his supervision. Not to forget my newly appointed main supervisor, Associate Professor Dr. Oo Chuan Wei for his kind guidance and support in my last year of candidature. I would also like to thank my co-supervisor Dr Wan Nazwanie Wan Abdullah for her emotional support and guidance. Special thanks to Dean, Professor Dr. Rohana Adnan and the staffs of School of Chemical Sciences for their supports and willingness in providing me the research facilities and services. I like to appreciate the opportunity given by the Dean of Institute of Postgraduate Studies for converting into PhD programme at Universiti Sains Malaysia. In addition, I would like to express my sincere gratitude to Professor Dr. Masato M. Ito, late Professor Dr. Akio Shimizu and Dr. Kazuyoshi Kaneko, from Soka University, Japan; Dr. Yoshiyuki Nakamura from Tokyo Institute of Technology, Japan as well as Professor Dr. Katsuaki Konishi and Associate Professor Dr. Yukatsu Shichibu from Hokkaido University, Japan for their valuable research assistance and guiding in analyses and special research programme. I like to thank my senior, Dr. Faridah Osman and my laboratory mates Ms. Nur Amanina Juniasari, Mrs. Syaza Atikah, Ms. Nur Fatin Liyana Salwadi and Ms. Siti Norhazwani for giving me happiness, sharing their knowledge and their great assistance throughout the completion of the programme. Last but not least, I would like to express my love and gratitude to my beloved soulmate and family for their physical, mental and emotional supports all the time. I love you.

## TABLE OF CONTENTS

<b>ACKNOWLEDGEMENT</b> .....	<b>ii</b>
<b>TABLE OF CONTENTS</b> .....	<b>iii</b>
<b>LIST OF TABLES</b> .....	<b>ix</b>
<b>LIST OF FIGURES</b> .....	<b>xii</b>
<b>LIST OF SCHEMES</b> .....	<b>xviii</b>
<b>LIST OF APPENDICES</b> .....	<b>xix</b>
<b>ABSTRAK</b> .....	<b>xxii</b>
<b>ABSTRACT</b> .....	<b>xxiv</b>
<b>CHAPTER 1 INTRODUCTION</b> .....	<b>1</b>
1.1 The fourth state of matter .....	1
1.2 Liquid crystals .....	1
1.3 Problem statements .....	4
1.4 Research objectives .....	6
1.5 Research scope .....	7
<b>CHAPTER 2 LITERATURE REVIEW</b> .....	<b>9</b>
2.1 History of liquid crystals .....	9
2.2 Classes of liquid crystals .....	10
2.2.1 Thermotropic liquid crystals .....	10
2.2.2 Lyotropic liquid crystals.....	11
2.3 Liquid crystal phases .....	11
2.3.1 Nematic phase .....	13
2.4 Non-linear disulphide centred liquid crystals.....	15
2.5 Factors affecting mesomorphic behavior .....	18
2.5.1 Linking groups .....	18
2.5.1(a) Azobenzene.....	19

2.5.1(b)	Schiff base .....	20
2.5.2	Flexible alkyl spacer.....	21
2.5.3	Substituent.....	22
2.6	Applications of liquid crystals.....	23
2.7	Molecular Model Study.....	26
2.8	Gold nanocomposites synthesized from liquid crystals and gold nanomaterial .....	27
<b>CHAPTER 3 METHODOLOGY.....</b>		<b>30</b>
3.1	Chemical reagents .....	30
3.2	Characterizations .....	30
3.2.1	Melting point.....	31
3.2.2	Colour.....	31
3.2.3	Elemental analysis.....	31
3.2.4	Fourier-transform infrared spectroscopy (FT-IR).....	31
3.2.5	Fourier-transform nuclear magnetic resonance (NMR).....	31
3.2.6	Ultraviolet-visible spectrophotometry (UV-Vis).....	32
3.2.7	Photoisomerization study .....	32
3.2.8	Optical texture analysis .....	32
3.2.9	Thermal analysis .....	33
3.2.10	Molecular model study.....	33
3.3	Synthesis.....	33
3.3.1	Synthesis of [Bis-6-(2-(6-(4-(4-acetylphenylazo)(phenoxy)-hexyloxy)phenoxy)alkyl)]disulphide, <b>Azo-SS-n</b> .....	33
3.3.1(a)	Synthesis of 4-(4-hydroxyphenylazo)acetophenone, <b>AzoOH</b> .....	35
3.3.1(b)	Synthesis of 6-bromo[4-(4-acetylphenylazo)phenoxy]hexane, <b>AzoBr</b> .....	36
3.3.1(c)	Synthesis of 2-[6-(4-(4-acetylphenylazo)phenoxy)-hexyloxy]phenol, <b>AzoPh</b> .....	36

3.3.1(d)	Synthesis of 2-[6-(4-(4-acetylphenylazo)phenoxy)-hexyloxy]phenoxybromoalkane, <b>Azo-Br-n</b> .....	37
3.3.1(e)	Synthesis of 6-[2-(6-(4-(4-acetylphenylazo)phenoxy)hexyloxy)phenoxy]alkylthioacetate, <b>Azo-ATA-n</b> .....	40
3.3.1(f)	Synthesis of 6-[2-(6-(4-(4-acetylphenylazo)phenoxy)hexyloxy)phenoxy]alkylthiol, <b>Azo-AT-n</b> .....	44
3.3.1(g)	Synthesis of [Bis-6-(2-(6-(4-(4-acetylphenylazo)phenoxy)hexyloxy)phenoxy)alkyl]disulphide, <b>Azo-SS-n</b> .....	47
3.3.2	Synthesis of [Bis-6-(2-((4-methoxyphenylimino)methyl)-5-(4'-hexyloxy-4-biphenyloxy)carbonyl)phenoxy)alkyl]disulphide, <b>SB-SS-n</b> .....	47
3.3.2(a)	Synthesis of 4'-hexyloxy-4-biphenylcarboxylic acid, <b>BPCOOH</b> .....	49
3.3.2(b)	Synthesis of 2-hydroxy-4-(4'-hexyloxy-4-biphenyloxy)carbonyl)benzaldehyde, <b>BPCHO</b> .....	50
3.3.2(c)	Synthesis of 2-(4-methoxyphenylimino)-5-(4'-hexyloxy-4-biphenyloxy)carbonyl)phenol, <b>SBPh</b> .....	50
3.3.2(d)	Synthesis of 2-(4-methoxyphenylimino)-5-(4'-hexyloxy-4-biphenyloxy)carbonyl)phenoxy-bromoalkane, <b>SB-Br-n</b> .....	51
3.3.2(e)	Synthesis of 6-[2-(4-methoxyphenylimino)-5-(4'-hexyloxy-4-biphenyloxy)carbonyl)phenoxy]-alkylthioacetate, <b>SB-ATA-n</b> .....	55
3.3.2(f)	Synthesis of 6-[2-(4-methoxyphenylimino)-5-(4'-hexyloxy-4-biphenyloxy)carbonyl)phenoxy]-alkylthiol, <b>SB-AT-n</b> .....	58
3.3.2(g)	Synthesis of [Bis-6-(2-(4-methoxyphenylimino)-5-(4'-hexyloxy-4-biphenyloxy)carbonyl)phenoxy)-alkyl]disulphide, <b>SB-SS-n</b> .....	61
3.3.3	Synthesis of [Bis-6-(2-(6-(4-(3-ethoxy-4-(4-methoxyphenylacetyloxy)benzylidene)phenoxy)hexyloxy)phenoxy)alkyl]disulphide, <b>E-SB-SS-n</b> .....	62
3.3.3(a)	Synthesis of 3-ethoxy-4-(4-methoxyphenylacetyloxy)benzaldehyde, <b>ECHO</b> .....	64
3.3.3(b)	Synthesis of 3-ethoxy-4-(4-methoxyphenylacetyloxy)benzylidene-4'-hydroxyaniline, <b>ESB</b> .....	64

3.3.3(c)	Synthesis of 6-bromo-[4-(3-ethoxy-4-(4-methoxy-phenylacetyloxy)benzylidene)phenoxy]hexane, <b>ESBBr</b> .....	65
3.3.3(d)	Synthesis of 2-[6-(4-(3-ethoxy-4-(4-methoxy-phenylacetyloxy)benzylidene)phenoxy)hexyloxy]-phenol, <b>ESBPh</b> .....	66
3.3.3(e)	Synthesis of 2-[6-(4-(3-ethoxy-4-(4-methoxy-phenylacetyloxy)benzylidene)phenoxy)hexyloxy]-phenoxybromoalkane, <b>E-SB-Br-n</b> .....	67
3.3.3(f)	Synthesis of 6-[2-(6-(4-(3-ethoxy-4-(4-methoxy-phenylacetyloxy)benzylidene)phenoxy)hexyloxy)-phenoxy]alkylthioacetate, <b>E-SB-ATA-n</b> .....	71
3.3.3(g)	Synthesis of 6-[2-(6-(4-(3-ethoxy-4-(4-methoxy-phenylacetyloxy)benzylidene)phenoxy)hexyloxy)-phenoxy]alkylthiol, <b>E-SB-AT-n</b> .....	74
3.3.3(h)	Synthesis of [Bis-6-(2-(6-(4-(3-ethoxy-4-(4-methoxyphenylacetyloxy)benzylidene)phenoxy)-hexyloxy)phenoxy)alkyl]disulphide, <b>E-SB-SS-n</b> .....	78
3.4	Synthesis and characterization of gold nanocomposite ( <b>GNC_LCx</b> ) from gold nanocluster ([Au <sub>25</sub> (SC <sub>12</sub> H <sub>25</sub> ) <sub>18</sub> ]TOA) and non-linear liquid crystal <b>SB-SS-n</b>	78
3.4.1	Chemical reagents .....	78
3.4.2	Characterizations .....	79
3.4.2(a)	Ultraviolet-visible spectrophotometry .....	79
3.4.2(b)	Transmission electron microscopy (TEM) .....	79
3.4.2(c)	Dynamic light scattering analysis (DLS).....	79
3.4.2(d)	Photoluminescence analysis (PL) .....	80
3.4.2(e)	Optical texture analysis.....	80
3.4.3	Synthesis.....	80
3.4.3(a)	Synthesis of non-linear LC oligomer, <b>SB-SS-n</b> .....	80
3.4.3(b)	Synthesis of gold nanocluster, [Au <sub>25</sub> (SC <sub>12</sub> H <sub>25</sub> ) <sub>18</sub> ]TOA .....	80
3.4.3(c)	Synthesis of gold nanocomposite, <b>GNC_LCx</b> .....	82
3.5	Research Flowchart .....	84
3.5.1	<b>Azo-SS-n, SB-SS-n and E-SB-SS-n</b> .....	84

3.5.2	<b>GNC_LCx</b> .....	87
<b>CHAPTER 4 RESULTS AND DISCUSSION.....</b>		<b>89</b>
4.1	[Bis-6-(2-(6-(4-(4-acetylphenylazo)phenoxy)hexyloxy)phenoxy)alkyl]- disulphide, <b>Azo-SS-n</b> .....	89
4.1.1	Physical characterization.....	89
4.1.2	Fourier-transform infrared spectroscopy (FT-IR).....	91
4.1.3	Fourier-transform nuclear magnetic resonance (FT-NMR).....	94
4.1.4	Ultraviolet visible spectrophotometry (UV-Vis).....	106
4.1.5	Optical texture and thermal analyses .....	107
	4.1.5(a) Structure-property relationship in <b>Azo-SS-n</b> .....	110
4.1.6	Molecular model study.....	114
4.1.7	Photoisomerization study .....	116
4.2	[Bis-6-(2-(4-methoxyphenylimino)-5-(4'-hexyloxy-4-biphenyloxy- carbonyl)phenoxy)alkyl]disulphide, <b>SB-SS-n</b> .....	121
4.2.1	Physical characterization.....	121
4.2.2	Fourier-transform infrared spectroscopy (FT-IR).....	123
4.2.3	Fourier-transform nuclear magnetic resonance (FT-NMR).....	125
4.2.4	Ultraviolet visible spectrophotometry (UV-Vis).....	138
4.2.5	Optical texture and thermal analyses .....	139
	4.2.5(a) Structure-property relationship in <b>SB-SS-n</b> .....	141
4.2.6	Molecular model study.....	145
4.2.7	Photoisomerization study .....	147
4.2.8	Gold nanocomposite, <b>GNC_LCx</b> .....	151
	4.2.8(a) UV-Vis spectrophotometry.....	152
	4.2.8(b) Transmission electron microscopy (TEM) .....	154
	4.2.8(c) Dynamic light scattering (DLS).....	155
	4.2.8(d) Photoluminescence study.....	157
	4.2.8(e) Optical texture analysis.....	159

4.2.8(f)	Summary .....	164
4.3	Bis-6-[2-(6-(4-(3-ethoxy-4-(4-methoxyphenylacetyloxy)benzylidene)-phenoxy)hexyloxy)phenoxy]alkyl]disulphide, <b>E-SB-SS-n</b> .....	166
4.3.1	Physical characterization .....	166
4.3.2	Fourier-transform infrared spectroscopy (FT-IR) .....	168
4.3.3	Fourier-transform nuclear magnetic resonance (FT-NMR) .....	170
4.3.4	Ultraviolet visible spectrophotometry (UV-Vis) .....	184
4.3.5	Optical texture and thermal analyses .....	185
4.3.5(a)	Structure-property relationship in <b>E-SB-SS-n</b> .....	188
4.3.6	Molecular model study .....	192
4.3.7	Photoisomerization study .....	194
4.4	Comparative analysis of <b>Azo-SS-n</b> , <b>SB-SS-n</b> and <b>E-SB-SS-n</b> .....	198
<b>CHAPTER 5 CONCLUSION AND FUTURE RECOMMENDATIONS....</b>		<b>202</b>
5.1	Conclusion .....	202
5.2	Recommendations for future research .....	204
<b>REFERENCES .....</b>		<b>205</b>
<b>APPENDICES</b>		

## LIST OF TABLES

	<b>Page</b>
Table 4.1	Molecular formula (MF), molecular weight (MW), percentage yield (%) and CHN microanalytical data of <b>Azo-SS-n</b> .....91
Table 4.2	Physical characteristics of <b>Azo-SS-n</b> .....91
Table 4.3	FT-IR absorption frequencies ( $\nu/\text{cm}^{-1}$ ) and relative intensities of <b>Azo-SS-n</b> .....94
Table 4.4	$^1\text{H}$ -NMR chemical shift ( $\delta/\text{ppm}$ ) of oligomers <b>Azo-SS-n</b> .....97
Table 4.5	$^1\text{H}$ - $^1\text{H}$ correlation as deduced from COSY experiment of <b>Azo-SS-6</b> .....98
Table 4.6	$^{13}\text{C}$ -NMR chemical shifts ( $\delta/\text{ppm}$ ) of oligomers <b>Azo-SS-n</b> .....101
Table 4.7	$^1\text{H}$ - $^{13}\text{C}$ correlations as inferred from the 2D HMQC and HMBC experiments for <b>Azo-SS-6</b> .....106
Table 4.8	Phase transition temperatures ( $^{\circ}\text{C}$ ), associated enthalpy and entropy change (kJ/mol) of titled oligomers <b>Azo-SS-n</b> .....110
Table 4.9	The properties obtained from optimized structures of <b>Azo-SS-n</b> after MM2 calculation.....116
Table 4.10	Duration of UV irradiation and thermal back relaxation required for <b>Azo-SS-n</b> and their respective conversion efficiency (CE) of <i>trans-cis-trans</i> photoisomerization. ....120
Table 4.11	Molecular formula (MF), molecular weight (MW), percentage yield (%) and CHN microanalytical data of <b>SB-SS-n</b> .....122
Table 4.12	Physical characteristics of <b>SB-SS-n</b> .....123
Table 4.13	FT-IR absorption frequencies ( $\nu/\text{cm}^{-1}$ ) and relative intensities of <b>SB-SS-n</b> .....125
Table 4.14	$^1\text{H}$ -NMR chemical shifts ( $\delta/\text{ppm}$ ) of oligomers <b>SB-SS-n</b> .....128

Table 4.15	$^1\text{H}$ - $^1\text{H}$ correlation as deduced from COSY experiment of <b>SB-SS-6</b> . .....	129
Table 4.16	$^{13}\text{C}$ -NMR chemical shifts ( $\delta/\text{ppm}$ ) of oligomers <b>SB-SS-n</b> .....	133
Table 4.17	$^1\text{H}$ - $^{13}\text{C}$ correlations as inferred from the 2D HMQC and HMBC experiments for <b>SB-SS-n</b> . ....	137
Table 4.18	Phase transition temperatures ( $^{\circ}\text{C}$ ), associated enthalpy (kJ/mol) and entropy change of titled oligomers <b>SB-SS-n</b> .....	141
Table 4.19	The properties obtained from optimized structures of <b>SB-SS-n</b> after MM2 calculation.....	146
Table 4.20	Duration of UV irradiation and thermal relaxation required for <b>SB-SS-n</b> . ....	151
Table 4.21	Transition temperatures of crystal-isotropic ( $T_{\text{Cr-I}}$ ), upon heating and isotropic-nematic ( $T_{\text{I-N}}$ ), nematic-crystal ( $T_{\text{N-Cr}}$ ), isotropic- crystal ( $T_{\text{I-Cr}}$ ), upon cooling of the respective <b>SB-SS-n</b> and <b>GNC_LCx</b> . ....	163
Table 4.22	Molecular formula (MF), molecular weight (MW), percentage yield (%) and CHN microanalytical data of <b>E-SB-SS-n</b> . ....	167
Table 4.23	Physical characteristics of <b>E-SB-SS-n</b> .....	168
Table 4.24	FT-IR absorption frequencies ( $\nu/\text{cm}^{-1}$ ) and relative intensities of <b>E-SB-SS-n</b> . ....	170
Table 4.25	$^1\text{H}$ -NMR chemical shifts ( $\delta/\text{ppm}$ ) of oligomers <b>E-SB-SS-n</b> .....	174
Table 4.26	$^1\text{H}$ - $^1\text{H}$ correlation as deduced from COSY experiment of <b>E-SB-SS-6</b> .....	175
Table 4.27	$^{13}\text{C}$ -NMR chemical shifts ( $\delta/\text{ppm}$ ) of oligomers <b>E-SB-SS-n</b> . ....	179
Table 4.28	$^1\text{H}$ - $^{13}\text{C}$ correlations as inferred from the 2D HMQC and HMBC experiments for <b>E-SB-SS-6</b> .....	184
Table 4.29	Phase transition temperatures ( $^{\circ}\text{C}$ ), associated enthalpy (kJ/mol) and entropy change of titled oligomers <b>E-SB-SS-n</b> .....	188

Table 4.30	The properties obtained from optimized structures of <b>E-SB-SS-n</b> after MM2 calculation.....	194
Table 4.31	Duration of UV irradiation and thermal relaxation required for <b>E-SB-SS-n</b> . ....	197

## LIST OF FIGURES

	<b>Page</b>
Figure 1.1	Molecular arrangement of solid, liquid crystal and liquid (Ghamsari & Carlescu, 2021). ..... 1
Figure 2.1	(a) Molecular organization and (b) symmetry (right) of the N phase. The rotational symmetry axis corresponds to the centre column of the molecular system. Rods and spiral imply the imaginary chirality of the molecule. The vertical symmetry indicates the axis of highest symmetry. The continuous ring of twofold axes represented the infinite number of twofold axes in the mirror plane of $D_{\infty h}$ (Lagerwall & Giesselmann, 2006). ..... 14
Figure 2.2	(a) Splay, (b) twist and (c) bend deformations (Ghamsari & Carlescu, 2021). ..... 15
Figure 3.1	Research workflow for the three series of LC oligomers, <b>Azo-SS-n</b> , <b>SB-SS-n</b> and <b>E-SB-SS-n</b> . ..... 86
Figure 3.2	Research workflow for the series of gold nanocomposites, <b>GNC_LCx</b> . ..... 88
Figure 4.1	FT-IR spectrum of representative oligomer <b>Azo-SS-6</b> . ..... 93
Figure 4.2	$^1\text{H-NMR}$ spectrum of oligomer <b>Azo-SS-6</b> . ..... 96
Figure 4.3	$^1\text{H-}^1\text{H}$ COSY spectrum of oligomer <b>Azo-SS-6</b> . ..... 98
Figure 4.4	$^{13}\text{C-NMR}$ spectrum of oligomer <b>Azo-SS-6</b> . ..... 100
Figure 4.5	$^{13}\text{C-NMR}$ DEPT90 spectrum of oligomer <b>Azo-SS-6</b> . ..... 102
Figure 4.6	$^{13}\text{C-NMR}$ DEPT135 spectrum of oligomer <b>Azo-SS-6</b> . ..... 102
Figure 4.7	$^1\text{H-}^{13}\text{C}$ HMQC spectrum of oligomer <b>Azo-SS-6</b> . ..... 105
Figure 4.8	$^1\text{H-}^{13}\text{C}$ HMBC spectrum of oligomer <b>Azo-SS-6</b> . ..... 105
Figure 4.9	UV-Vis absorption spectra of <b>Azo-SS-n</b> in chloroform. .... 107

Figure 4.10	DSC trace of representative <b>Azo-SS-6</b> during heating and cooling cycles at $\pm 2.0$ °Cmin <sup>-1</sup> . .....	108
Figure 4.11	Photomicrographs for <b>Azo-SS-n</b> (10X magnification; scale bar = 50.00 $\mu$ m). (a) <b>Azo-SS-6</b> shows the nematic droplets with four-point brush defects at 99.1 °C. (b) <b>Azo-SS-7</b> formed nematic fern leaved texture at 151.0 °C. (c) Wave texture by <b>Azo-SS-8</b> at 110.6 °C. (d) Cone with four brushes by <b>Azo-SS-9</b> at 98.0 °C. (e) Tiny cylinders with droplets of nematic phase by <b>Azo-SS-10</b> at 67.5 °C. (f) Clover leaves with four brushes texture by <b>Azo-SS-11</b> at 68.2 °C.....	109
Figure 4.12	Dependence of the transition temperatures on the number of carbon atoms, n in inner alkyl spacer of the oligomers <b>Azo-SS-n</b> upon heating and cooling at $\pm 2.0$ °Cmin <sup>-1</sup> .....	112
Figure 4.13	Molecular models I and II show the all- <i>trans</i> -conformation for <b>Azo-SS-6</b> and <b>Azo-SS-7</b> , respectively. Molecular model III shows the linear conformation for <b>Azo-SS-6</b> while molecular model IV shows the bent conformation for <b>Azo-SS-7</b> . S-S linking group is shown as the central yellow balls. All the mesogenic units remain anti-parallel. ....	112
Figure 4.14	Dependence of the entropy change associated with the isotropic-nematic transition, $\Delta S_{I-N}/R$ on the length of the inner alkyl spacers, n, for the oligomers <b>Azo-SS-n</b> . ....	114
Figure 4.15	Absorption spectra of <b>Azo-SS-9</b> with different exposure time of UV light. 0 min represents the absence of UV light. ....	117
Figure 4.16	Time-dependent photoisomerization curve of oligomer <b>Azo-SS-9</b> showing the <i>trans</i> -isomer in the presence of UV irradiation within 12 minutes. ....	117
Figure 4.17	Thermal back relaxation process for the oligomer <b>Azo-SS-9</b> showing that the <i>cis</i> -to- <i>trans</i> isomerisation completely occurred within 600 minutes.....	118

Figure 4.18	Time-dependence photoisomerization curve of <i>cis</i> -isomer displaying thermal back relaxation time. ....	119
Figure 4.19	FT-IR spectrum of representative oligomer <b>SB-SS-6</b> . ....	124
Figure 4.20	<sup>1</sup> H-NMR spectrum of oligomer <b>SB-SS-6</b> . ....	127
Figure 4.21	<sup>1</sup> H- <sup>1</sup> H COSY spectrum of oligomer <b>SB-SS-6</b> . ....	129
Figure 4.22	<sup>13</sup> C-NMR spectrum of oligomer <b>SB-SS-6</b> . ....	132
Figure 4.23	<sup>13</sup> C-NMR DEPT90 spectrum of oligomer <b>SB-SS-6</b> . ....	134
Figure 4.24	<sup>13</sup> C-NMR DEPT135 spectrum of oligomer <b>SB-SS-6</b> . ....	134
Figure 4.25	<sup>1</sup> H- <sup>13</sup> C HMQC spectrum of oligomer <b>SB-SS-6</b> . ....	136
Figure 4.26	<sup>1</sup> H- <sup>13</sup> C HMBC spectrum of oligomer <b>SB-SS-6</b> . ....	137
Figure 4.27	UV-Vis absorption spectra of oligomers <b>E-SB-SS-n</b> in chloroform. ....	138
Figure 4.28	DSC trace of representative <b>SB-SS-7</b> during heating and cooling cycles at $\pm 2.0$ °Cmin <sup>-1</sup> . ....	140
Figure 4.29	Photomicrographs for oligomer <b>SB-SS-n</b> (10X magnification, scale bar = 50.00 $\mu$ m). Nematic Schlieren texture with brush defect exhibited by (a) <b>SB-SS-6</b> at 190.1 °C, (b) <b>SB-SS-7</b> at 188.3 °C. (c) Schlieren texture coalescent with crystal forming by <b>SB-SS-8</b> at 183.8 °C. Nematic Schlieren texture with two and four-point brush defects exhibited by (d) <b>SB-SS-9</b> at 178.9 °C and (e) <b>SB-SS-10</b> at 169.2 °C. (f) Nematic Schlieren texture with four-point brush defect shown by <b>SB-SS-11</b> at 164.5 °C. ....	141
Figure 4.30	Dependence of the transition temperatures on the number of carbon atoms, n in inner alkyl spacer of the oligomers <b>SB-SS-n</b> upon heating and cooling at $\pm 2.0$ °Cmin <sup>-1</sup> . ....	143
Figure 4.31	Molecular models I and II show the all- <i>trans</i> -conformation for <b>SB-SS-6</b> and <b>SB-SS-7</b> , respectively. Model III shows the bent conformation for <b>SB-SS-6</b> while model IV shows the stretched conformation for <b>SB-SS-7</b> . S-S linking group is shown as the central yellow balls. ....	144

Figure 4.32	Dependence of the entropy change associated with the isotropic-nematic transition, $\Delta S_{I-N}/R$ on the number of carbon atoms in inner alkyl spacer, $n$ for the titled oligomers <b>SB-SS-n</b> .....	145
Figure 4.33	Absorption spectra of <b>SB-SS-7</b> with different exposure time of UV light. 0 min represents the absence of UV light. ....	148
Figure 4.34	Time-dependent photoisomerization curve of oligomer <b>SB-SS-7</b> showing the <i>trans</i> -isomer in the presence of UV irradiation within 13 minutes. ....	148
Figure 4.35	Thermal back relaxation process for the oligomer <b>SB-SS-7</b> showing that the <i>cis</i> -to- <i>trans</i> isomerization completely within 1200 minutes. ....	149
Figure 4.36	Time-dependence photoisomerization curve of <i>cis</i> -isomer displaying thermal back relaxation time. ....	150
Figure 4.37	Postulated structure of nanocomposite, <b>GNC_LCx</b> . ....	152
Figure 4.38	UV-Vis measurement of the dissolved samples with concentration of 0.1 mM at room temperature. (a) <b>Au<sub>25</sub></b> . (b) <b>SB-SS-n</b> . (c) <b>GNC_LCx</b> . ....	154
Figure 4.39	TEM images (scale bar = 20.00 nm) of the (a) <b>Au<sub>25</sub></b> . (b) Representative <b>GNC_LC11</b> .....	154
Figure 4.40	DLS measurement of dissolved samples with concentration of 0.5 mM at room temperature. (a) <b>Au<sub>25</sub></b> . (b) <b>SB-SS-n</b> . (c) <b>GNC_LCx</b> ...	156
Figure 4.41	Odd-even effect. (a) Graph of size against number of methylene units within inner alkyl spacer in the series of <b>SB-SS-n</b> . (b) Graph of size against number of methylene units within inner alkyl spacer in the series of <b>GNC_LCx</b> . ....	157
Figure 4.42	Photoluminescence study on (a-b) <b>Au<sub>25</sub></b> , (c-d) <b>SB-SS-n</b> and (e-f) <b>GNC_LCx</b> . Left: Emission spectra; Right: Excitation spectra. ....	159
Figure 4.43	The POM micrographs showing the nematic Schlieren texture by representative <b>SB-SS-n</b> and <b>GNC_LCx</b> at respective temperatures (10X magnification, scale bar = 50.00 $\mu\text{m}$ ). (a) <b>SB-SS-9</b> at 188.3	

	°C. (b) <b>GNC_LC9</b> at 168.6 °C. (c) <b>SB-SS-10</b> at 169.3 °C. (d) <b>GNC_LC10</b> at 140.0 °C. (e) <b>SB-SS-11</b> at 164.5 °C. (f) <b>GNC_LC11</b> at 144.2 °C. ....	162
Figure 4.44	Transition temperatures of crystal-isotropic ( $T_{C-I}$ ), isotropic-nematic ( $T_{I-N}$ ) and nematic-crystal ( $T_{N-Cr}$ ) of the respective <b>SB-SS-n</b> and mesogenic <b>GNC_LCx</b> as well as isotropic-crystal ( $T_{I-Cr}$ ) of the respective non-mesogenic <b>GNC_LCx</b> .....	164
Figure 4.45	FT-IR spectrum of representative oligomer <b>E-SB-SS-6</b> .....	169
Figure 4.46	$^1\text{H}$ -NMR spectrum of oligomer <b>E-SB-SS-6</b> .....	173
Figure 4.47	$^1\text{H}$ - $^1\text{H}$ COSY spectrum of oligomer <b>E-SB-SS-6</b> .....	175
Figure 4.48	$^{13}\text{C}$ -NMR spectrum of oligomer <b>E-SB-SS-6</b> .....	178
Figure 4.49	$^{13}\text{C}$ -NMR DEPT90 spectrum of oligomer <b>E-SB-SS-6</b> . ....	180
Figure 4.50	$^{13}\text{C}$ -NMR DEPT135 spectrum of oligomer <b>E-SB-SS-6</b> . ....	180
Figure 4.51	$^1\text{H}$ - $^{13}\text{C}$ HMQC spectrum of oligomer <b>E-SB-SS-6</b> . ....	183
Figure 4.52	$^1\text{H}$ - $^{13}\text{C}$ HMBC spectrum of oligomer <b>E-SB-SS-6</b> .....	183
Figure 4.53	UV-Vis absorption spectra of oligomers <b>E-SB-SS-n</b> in chloroform. ....	185
Figure 4.54	DSC trace of representative <b>E-SB-SS-10</b> during heating and cooling cycles at $\pm 2.0$ °Cmin $^{-1}$ . ....	187
Figure 4.55	Photomicrographs for oligomers <b>E-SB-SS-n</b> showing the respective nematic phase (10X magnification, scale bar = 50.00 $\mu\text{m}$ ). Nematic droplets by (a) <b>E-SB-SS-6</b> at 211.9 °C and (b) <b>E-SB-SS-7</b> at 219.7 °C. (c) Marble texture by <b>E-SB-SS-8</b> at 174.9 °C. (d) Nematic droplets by <b>E-SB-SS-9</b> at 220.0 °C. (e) Marble texture and Schlieren texture by <b>E-SB-SS-10</b> at 219.7 °C. (f) Nematic droplets by <b>E-SB-SS-11</b> at 204.6 °C. ....	188
Figure 4.56	Dependence of the transition temperatures on the number of carbon atoms, n in inner alkyl spacer of the oligomers <b>E-SB-SS-n</b> upon heating and cooling at $\pm 2.0$ °Cmin $^{-1}$ .....	190

Figure 4.57	Molecular models I and II show the all- <i>trans</i> -conformation for <b>E-SB-SS-6</b> and <b>E-SB-SS-7</b> , respectively. Model III shows the bent conformation for <b>E-SB-SS-6</b> with 86.0 ° as the dihedral angle of C-S-S-C while model IV shows the stretched conformation for <b>E-SB-SS-7</b> with 93.2 ° as the dihedral angle of C-S-S-C. S-S linking group is shown as the central yellow balls. ....	191
Figure 4.58	Dependence of the entropy change associated with the isotropic-nematic transition, $\Delta S_{I-N}/R$ on the number of carbon atoms in inner alkyl spacer, n for the titled oligomers <b>E-SB-SS-n</b> .....	192
Figure 4.59	Absorption spectra of <b>E-SB-SS-6</b> with different exposure time of UV light. 0 min represents the absence of UV light. ....	195
Figure 4.60	Time-dependent photoisomerization curve of oligomer <b>E-SB-SS-6</b> showing the <i>trans</i> -isomer, in the presence of UV irradiation within 16 minutes. ....	195
Figure 4.61	Thermal back relaxation process for the oligomer <b>E-SB-SS-6</b> showing that the <i>cis</i> -to- <i>trans</i> isomerization completely within 780 minutes. ....	196
Figure 4.62	Time-dependence photoisomerization curve of <i>cis</i> -isomer displaying thermal back relaxation time. ....	196

## LIST OF SCHEMES

	<b>Page</b>
Scheme 3.1 Synthesis route for the preparation of non-linear LC oligomers, <b>Azo-SS-n</b> .....	34
Scheme 3.2 Synthesis route for the preparation of non-linear LC oligomers, <b>SB-SS-n</b> .....	48
Scheme 3.3 Synthesis route for the preparation of non-linear LC oligomers, <b>E-SB-SS-n</b> .....	63
Scheme 3.4 Synthesis route for the preparation of gold nanocluster, <b>Au25</b> . .....	81
Scheme 3.5 Synthesis route for the preparation of gold nanocomposites, <b>GNC_LCx</b> .....	83

## LIST OF APPENDICES

°C	Degree Celcius
°Cmin <sup>-1</sup>	Degree Celcius per minute
ΔH	Enthalpy change
ΔS <sub>I-N/R</sub>	Entropy change associated with transition of isotropic-nematic per gas constant
%	Percentage
<sup>1</sup> H-NMR	Proton nuclear magnetic resonance
<sup>13</sup> C-NMR	Carbon-13 nuclear magnetic resonance
ATR	Attenuated total reflectance
Bn	Banana phase
BP	Blue phase
Br	Bromide ion
Br(CH <sub>2</sub> ) <sub>n</sub> Br	Dibromoalkane
Br(CH <sub>2</sub> ) <sub>6</sub> Br	1,6-Dibromohexane
CDCl <sub>3</sub>	Deuterated chloroform
CE	Conversion efficiency
CH <sub>3</sub> COS <sup>-</sup> K <sup>+</sup>	Potassium thioacetate
CHCl <sub>3</sub>	Chloroform
CHN	Carbon, hydrogen and nitrogen
COSY	Correlated spectroscopy
Cl	Chloride ion
cm	centimeter
Col	Columnar phase
DCC	<i>N,N'</i> -Dicyclohexylcarbodiimide
DCM	Dichloromethane
DEPT	Distortionless enhancement by polarization transfer
DLS	Dynamic light scattering study
DMAP	4-Dimethylaminopyridine
DMF	Dimethylformamide
DSC	Differential scanning calorimetry
EtOH	Ethanol
FT-IR	Fourier-transform infrared

FT-NMR	Fourier-transform nuclear magnetic resonance
g	Gram
GNC	Gold nanocluster
HC=N	Azomethine; Schiff base
H <sub>2</sub> O <sub>2</sub>	Hydrogen peroxide
HAuCl <sub>4</sub>	Chloroauric acid
HCl	Hydrochloric acid
HMBC	Heteronuclear multiple-bond coherence
HMQC	Heteronuclear multiple-quantum correlation
I	Iodide ion
J	Coupling constant
K <sub>2</sub> CO <sub>3</sub>	Potassium carbonate
KI	Potassium iodide
kJmol <sup>-1</sup>	Kilojoule per mole
KOH	Potassium hydroxide
kPa	Kilopascal
LC(s)	Liquid crystal(s)
LCD	Liquid crystal display
L/D ratio	Length-to-breadth ratio; aspect ratio
m	Medium intensity
M	Molar
MF	Molecular formula
min	Minute
MW	Molecular weight
mL	Milliliter
mmol	Millimole
n	Number of carbons in the inner alkyl spacer
n	Director
N	Nematic phase
N*	Chiral nematic phase
Na <sub>2</sub> S <sub>2</sub> O <sub>5</sub>	Sodium metabisulfite
NaI	Sodium iodide
NaNO <sub>2</sub>	Sodium nitrite
NaOH	Sodium hydroxide

nm	Nanometer
N=N	Azobenzene
NMR	Nuclear magnetic resonance
N <sub>TB</sub>	Twist-bend nematic phase
PL	Photoluminescence
POM	Polarized optical microscopy
pH	Potential of Hydrogen
s	Strong intensity
S-S	Disulphide linkage
Sm	Smectic phase
T <sub>c</sub>	Clearing temperature
T <sub>Cr-I</sub>	Crystal-to-isotropic transition temperature
T <sub>I-Cr</sub>	Isotropic-to-crystal transition temperature
T <sub>I-N</sub>	Isotropic-to-nematic transition temperature
T <sub>m</sub>	Melting temperature
T <sub>N-Cr</sub>	Nematic-to-crystal transition temperature
TEM	Transmission electron microscopy
TGB	Twist grain boundary phase
THF	Tetrahydrofuran
TMS	Tetramethylsilane
TOAB	Tetraoctylammonium bromide
UV	Ultraviolet
UV-Vis	Ultraviolet visible
W	Watt

**SINTESIS, PENCIRIAN, SIFAT MESOMORFIK DAN KAJIAN MODEL  
MOLEKUL BAGI OLIGOMER HABLUR CECAIR BUKAN LINEAR YANG  
BERPUSATKAN DISULFIDA**

**ABSTRAK**

Tiga siri oligomer hablur cecair bukan linear yang berpusatkan disulfida, iaitu **Azo-SS-n**, **SB-SS-n** dan **E-SB-SS-n** telah berjaya disintesis dan dicirikan. **Azo-SS-n** mempunyai unit azo (N=N) dan tidak mempunyai substituen sisi manakala **SB-SS-n** dan **E-SB-SS-n** mempunyai unit azomethine (HC=N) dan substituen sisi masing-masing. Penjelasan struktur sebatian adalah berdasarkan kaedah spektroskopi seperti CHN, FT-IR, 1D dan 2D-NMR serta UV-Vis manakala sifat mesomorfik dan kelakuan terma mereka dianalisis oleh POM dan DSC. Ketiga-tiga siri adalah nematogen monotropik. Dalam kajian fotoisomerisasi, **Azo-SS-n** mempunyai nilai CE tinggi (>80.00 %) manakala **SB-SS-n** dan **E-SB-SS-n** mempunyai nilai CE sederhana (>40.00 %). Walaubagaimanapun, ketiga-tiga siri telah menunjukkan tempoh kelonggaran belakang terma yang panjang dan mencadangkan potensi mereka dalam penciptaan peranti storan optik. Pengiraan MM2 dijalankan untuk memperolehi struktur molekul, kepanjangan, kelebaran, nisbah aspek dan sudut kilasan C-S-S-C. Sifat geometri teori tersebut digunakan untuk menyokong hubungan struktur-sifat eksperimen siri masing-masing. Nilai entalpi **SB-SS-n** yang rendah menunjukkan potensi dalam menghasilkan eutektoid. Oleh itu, **SB-SS-n** telah dipilih untuk berdop dengan nanokluster aurum [Au<sub>25</sub>(SC<sub>12</sub>H<sub>25</sub>)<sub>18</sub>]TOA supaya mensintesis nanokomposit aurum dan didapati bahawa **GNC\_LCx** mempunyai peningkatan sifat fotoluminasi dengan kehadiran **SB-SS-n**. Dalam kajian tekstur optik, **GNC\_LCx** yang panjang (x=9, 10, 11) adalah nematik dan monotropik semasa disejukkan serta menunjukkan

suhu peralihan yang lebih tinggi daripada perumah tidak terdop **SB-SS-n** masing-masing.

**SYNTHESIS, CHARACTERIZATION, MESOMORPHIC PROPERTIES  
AND MOLECULAR MODEL STUDY OF NON-LINEAR DISULPHIDE  
CENTRED LIQUID CRYSTAL OLIGOMERS**

**ABSTRACT**

Three series of non-linear disulphide centred liquid crystal oligomers, namely **Azo-SS-n**, **SB-SS-n** and **E-SB-SS-n** were successfully synthesized and characterized. **Azo-SS-n** has azo unit (N=N) and no lateral substituent whereas **SB-SS-n** and **E-SB-SS-n** have azomethine (HC=N) and respective lateral substituents. The structural elucidation of the compounds was based on the spectroscopic methods such as CHN, FT-IR, 1D and 2D-NMR and UV-Vis whereas their optical texture and thermal behaviours were analysed by POM and DSC, respectively. All three series are predominantly monotropic nematogen. In the photoisomerization study, **Azo-SS-n** has high CE values (>80.00 %) whereas **SB-SS-n** and **E-SB-SS-n** have moderate CE values (>40.00 %). Though, three series showed long duration of thermal back relaxation which suggested their potential in the creation of optical storage devices. MM2 calculation is conducted to obtain the molecular conformation, molecular length and breadth, aspect ratio and C-S-S-C torsion angle. The theoretical geometrical properties obtained are used to support the experimental structure-property relationship of the series. The low enthalpy values of **SB-SS-n** showed its potential in producing eutectoid. Hence **SB-SS-n** has chosen to be doped with gold nanocluster [Au<sub>25</sub>(SC<sub>12</sub>H<sub>25</sub>)<sub>18</sub>]TOA and it is observed that the **GNC\_LCx** has enhanced photoluminescence property with the presence of **SB-SS-n**. In the optical texture analysis, the longer **GNC\_LCx** (x=9, 10, 11) are monotropically nematic upon cooling with higher transition temperatures than their respective undoped host **SB-SS-n**.

# CHAPTER 1

## INTRODUCTION

### 1.1 The fourth state of matter

Liquid crystals (LCs) are soft condensed materials that cannot be simply classified as solid or liquid. Despite being the intermediary state between solids and liquids, the LCs are thermodynamically stable as the solids, liquids and gases. Hence, they are known as the fourth state of matter. The molecular arrangement of solid, LC and liquid is depicted in Figure 1.1.

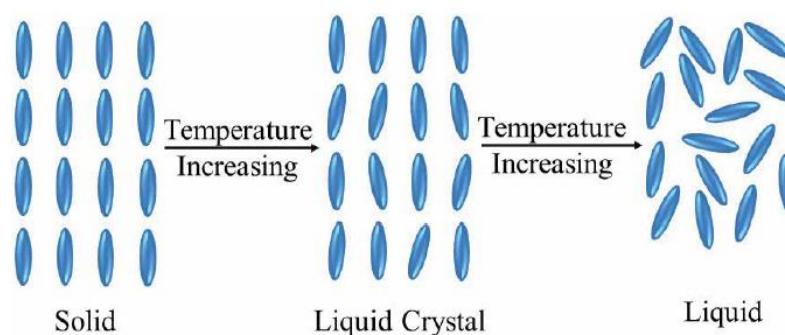


Figure 1.1 Molecular arrangement of solid, liquid crystal and liquid (Ghamsari & Carlescu, 2021).

### 1.2 Liquid crystals

LC has been defined in many ways since its discovery in the 19<sup>th</sup> century. It is regarded as the fourth state of matter that is unique and exists as an intermediary state between three-dimensional crystalline solids and ordinary liquids (Iskandar, Yeap, Maeta, et al., 2024). Hence, the LCs are also known as the soft condensed materials (Gray, 1998; Iskandar et al., 2020; Malik et al., 2022). LCs are sometimes known as mesomorphic systems and other entities such as molecule aggregates and nanoparticles consisting a unique entity. The entities that are capable of exhibiting the mesomorphic phase are referred as mesogens, mesogenic substance or anisometric molecules (Lagerwall & Scalia, 2012; Rahman, Sarkar, et al., 2015). The exhibition of liquid

crystalline behaviour from a compound is heavily dependent on the molecular structures as it must consist of a mesogenic central core, flexible linking spacer, lateral and terminal groups. Three important elements in the molecular structures usually consist of a planar and rigid aromatic rings, double bonds and polarizable groups (Ghamsari & Carlescu, 2021). The researchers are investigating the intermolecular interactions, charge-transfer systems and hydrogen-bonded systems based on the different molecular structures which result in a variety of mesomorphic behaviours (Yoshizawa, 2012).

The mesogen can be in any shape as long as it is flexible enough to promote the self-assembly of the LC structure (Ooi et al., 2013). The aromatic ring can affect the electrical and elastic properties of a LC due to its short-range molecular force; the linking spacers can stabilize the LC against external stimuli such as the UV radiation, moisture and chemicals; the terminal group helps to determine the dielectric constant and anisotropy of the LC; and the lateral group can affect the elastic energy and phase transition temperature of the LC (Ahmed et al., 2019; Ghamsari & Carlescu, 2021).

LC dimer is the simplest class of oligomers which contain two mesogenic units connecting through a single spacer. When the molecules are incorporated with at least two mesogenic units connected through flexible spacer, they are known as LC oligomers such as trimer, tetramer and so on (Lee et al., 2012; Mohammad et al., 2016). LC dimers are fascinating as they possess different chemical and physical properties from the conventional LCs with low molecular mass. The LC dimers are highly dependent on the length and parity of the flexible spacer (Yoshizawa, 2012). The dimers have a typical behaviour of showing the pronounced alternations or so called the odd-even effect on transitional properties when they have varying number of methylene moieties in the flexible spacer (Tufaha et al., 2023). The very first series of LC dimer was investigated by Pal et al. (2007). They found the dimers with longer alkyl spacers

have a high tendency to exhibit smectic behaviour. On the contrary, the dimers with short alkyl spacer showed an unexpected odd-even effect on the I-N transition. Meanwhile, oligomers are reported to have different mesomorphic behaviours from their corresponding monomers (Yeap et al., 2017). For example, the monomers have lower clearing point and less dependent on the spacer length and parity than the oligomers do (Imrie & Luckhurst, 1998).

LC oligomers can be categorized into linear and non-linear forms. Representative linear LCs are the dimers (Osman et al., 2014), trimers (Tuchband et al., 2019; Yeap et al., 2009), tetramers (Henderson & Imrie, 2005a; Yao et al., 2016), pentamers (Hattori et al., 2022; Yelamaggad et al., 2007) and hexamers (Blumstein & Stickles, 1982; Simpson et al., 2017). The study on oligomeric LCs are interesting as they are capable of forming the supramolecular assemblies (Ogasawara et al., 2008). Distinctive odd-even effect is often spotted in the transitional properties exhibited by the linear LCs with varied spacer lengths. Whilst for the non-linear oligomers, they promoted different ordering in the mesomorphic phases and have one spacer group connected laterally. Examples of them are dendrimers (Aya et al., 2021), U-shaped (Rahman, Sarkar, et al., 2015), Y-shaped (Yoshizawa et al., 2006),  $\lambda$ -shaped (Yamaguchi et al., 2005), H-shaped (Sayama et al., 2019), S-shaped (Osman et al., 2016) and V-shaped (Salwadi et al., 2023). There are also other types of LCs such as the metallomesogen in which a metal is incorporated in the mesomorphic system and ionic LCs which contains anions and cations (Binnemans, 2005).

In terms of molecular structure based on the symmetry, the LC oligomers can also be divided into symmetrical LCs which have the same mesogenic units and non-symmetrical LCs which have different mesogenic units (Henderson & Imrie, 2005a). In the present work, the three targeted series of LCs can also be considered as

symmetrical twins as two similar mesogenic units are connected through the inner and outer flexible linking spacers. This type of LC is usually found to possess much higher melting temperature ( $T_m$ ) and clearing temperature ( $T_c$ ) than the single rod-like LCs.  $T_m$  specifies the melting of crystalline state and  $T_c$  specifies the transition into isotropic liquid (Lagerwall & Scalia, 2012). In addition, the high temperature somehow diminish the mesogeneity of the molecule in some cases (Griffin et al., 1981; Griffin et al., 1976).

### **1.3 Problem statements**

Despite the pioneering report by Pal et al. in 2007, there remains a notable scarcity of studies on the disulphide (S-S) centred LC oligomers. Previous research predominantly focused on non-linear LC oligomers centred with biphenyl, alkyl or alkoxy spacer, with only a few comprehensive documentations on the non-linear S-S bridged variants (Kundu et al., 2009, 2010; Lee et al., 2012; Osman et al., 2014; Yeap et al., 2014). The S-S bond is stable but can easily be restructured due to the soft and highly polarizable sulphur atoms, particularly under conditions such as heating, mechanical stress or photochemical reaction (Huang et al., 2021).

Dimers containing S-S has an unique property as the presence of S-S ensures a molecular curvature exists in the molecular structure (Tufaha et al., 2023). The molecular curvature and dimer with odd-membered spacer are the critical prerequisites for the exhibition of the unique mesophases, especially the recently discovered twist-bend nematic phase (Alshammari et al., 2022; Arakawa, Ishida, et al., 2021; Pocięcha et al., 2021; Walker et al., 2021). However, the majority of studies have focused on the dimers equipped with biphenyl, cyanobiphenyl, alkyl and alkoxy groups. Other factors, such as linking group, functional group, terminal chain and mesogenic type have not been explored in depth. This research gap is particularly important in the context of the twist-bend nematic phase, which has been applied to various applications

such as the photonic and switchable optical devices, liquid crystalline gel system, photoalignment technologies and the elastic bodies (Arakawa, Komatsu, et al., 2021; Feng et al., 2020; Mrukiewicz et al., 2019; Sridurai et al., 2019).

It is known that the transitional properties of the LC dimers significantly depend on the length and parity of the flexible spacer, which influence the molecular anisotropy and relative orientation of the mesogenic unit and therefore LC will have different conformers depending on the parity of the flexible spacer. The literature suggests that increasing alkyl spacer length has higher tendency to exhibit a smectic phase (Henderson & Imrie, 2005b; Osman et al., 2014). For instance, the S-S centred alkoxyphenyl dimers by Pal et al. (2007) exhibited both nematic and smectic phases except the one with the shortest spacer only showed monotropic nematic phase.

A notable research gap in the literature review is the limited consideration of lateral substituents in the design of S-shaped S-S bridges LC oligomers. In general, the lateral substituents can significantly influence molecular structure and transitional properties by broadening the molecular shape, which subsequently lower the thermal stability of the mesomorphic system (Ahmed et al., 2019; Berdagué et al., 1993; Demus, 1998; Imrie & Luckhurst, 1998). The elongated lateral chain causes an increased aspect ratio or length-to-breadth (L/D) ratio and thus having lower thermal stability. Additionally, large lateral substituents such as bulky rings may cause the molecule to behave more like a rod-like mesogen, complicating the prediction of mesomorphic behaviour.

The previous synthesized series of S-shaped oligomers were mostly attached with terminal halogen group. It has been showing the polarizability of the halogens can disrupt the molecular packing and induced the mesomorphic behaviour at low  $T_c$ . Yeap et al. (2017) studied the effect of terminal substituent and concluded that the series with

terminal non-halogen group had higher  $T_c$  and higher nematic stability than the series with terminal halogen group. It is hypothesized that S-S centred oligomers with terminal non-halogen group and long alkyl spacers may induce polymorphic behaviour with low  $T_m$  but high  $T_c$ .

Linking groups such as azo (N=N) and azomethine (HC=N) offer additional opportunities in altering molecular linearity and rigidity. They can restrict the molecular rotation due to their double-bond nature and their ability to undergo *trans-cis-trans* isomerization may be relevant for non-display application such as optical storage devices.

The present study aims to address these gaps in the understanding of non-linear LC oligomers, particularly those with S-S linkages. We will investigate the effects of varying inner alkyl spacers and constrained outer alkyl spacers, terminal non-halogen group, linking groups like N=N and HC=N as well as the lateral substituents on mesomorphic properties. Additionally, photoisomerization studies will be conducted to explore their ability for *trans-cis-trans* isomerization. Molecular model analysis will help understand the structure-property relationships and their impact on mesomorphic behaviour. Ultimately, the research seeks to advance our knowledge of S-S centred LC oligomers and their potential applications in optical storage and other advanced technologies.

#### **1.4 Research objectives**

Three series of non-linear LC oligomers with different mesogenic units and lateral substituent have been synthesized. The objectives of the present work are:

- a) To synthesize, characterize and investigate the liquid crystalline properties of three novel series of non-linear S-S centred LC oligomers with different mesogenic units and lateral substituent.

- b) To carry out photoisomerization study on the three series of LC oligomers with respective N=N and HC=N moieties using UV irradiation and thermal back relaxation methods.
- c) To carry out molecular model study using MM2 calculation to obtain the optimized molecular structures and geometrical parameters of the three series of LC oligomers.
- d) To study the structure-property relationship of the three series of LC oligomers and make the comparative analysis among the three series.
- e) To identify the series that has the potential to dope with the gold nanocluster for property enhancement.

## **1.5 Research scope**

The scope for this entire work is to confine to the study of three series of S-S bridged LC oligomers with desirable substituents, inner alkyl spacer varied from six to eleven carbons, outer alkyl spacer retained at six carbons and a terminal alkyl group. The series of LC oligomers will be first synthesized and characterized to confirm their molecular structures based on the FT-IR, 1D and 2D-NMR, CHN and UV-Vis. The mesomorphic behaviour including the thermal property of the LC oligomers will be analysed by using the POM and DSC, respectively. Photoisomerization study will be conducted on the titled oligomers by using UV irradiation and thermal back relaxation methods to study their photoswitching property. Molecular model studies and theoretical information calculated from the MM2 calculation will be used to aid in explaining the results obtained.

The overall organizational structure of the thesis consist of five chapters and each chapter provides detailed information on research interest as stated in the research objectives in the previous section 1.3. Chapter 1 is an introduction that addresses a

general overview of the fourth state of matter, LCs, problem statements, research objectives and research scope. Chapter 2 starts with the history of LCs and describes the classes of LCs, the non-linear S-S centred LC oligomers, the types of LC phase, factors affecting mesomorphic behaviour and the applications of LCs. The literature review on the non-linear S-S centred oligomers is discussed as well to learn the research gap in this research topic. A novel series of gold nanocomposite synthesized from the non-linear S-S bridged LCs and gold nanocluster is presented in this work as a supplementary work. Hence, the general overview of the gold nanocomposite is included in the chapter. Molecular model study is covered in the chapter to provide an overview and the benefit of utilising the computational calculation in the research. Chapter 3 is devoted to describe the chemical reagents used as well as procedures to carry out the synthesis and characterizations of the three series of LC oligomers, gold nanocluster and the series of gold nanocomposites. Chapter 4 encloses the results and discussion for all series of LC oligomers to understand the fundamental characterizations, optical texture and thermal analyses, the photoisomerization study, the molecular model study and the structure-property relationship. The results and discussions and conclusion on the gold nanocluster and gold nanocomposites are also covered in the chapter. A comparison of the mesomorphic behaviours among the three series is carried out and highlighted in the last section of the chapter. It helps to get better understanding of their difference in terms of molecular structures with respective constituted mesogenic moieties and discuss how the variety can lead to respective distinguishable mesomorphic and thermal behaviours, photoisomerization property and optimized molecular structures obtained. Lastly, Chapter 5 includes the conclusion of the present work about the non-linear S-S bridged LC oligomers and the recommendations for future research.

## **CHAPTER 2**

### **LITERATURE REVIEW**

#### **2.1 History of liquid crystals**

The discovery of LCs was officially recognized in 1888 when the Prague botanist Friedrich Reinitzer observed the uncommon behaviour of cholesterol benzoate, which showed double melting points at 145.5 and 178.5 °C (Dierking, 2022; Gray, 1998; Lagerwall & Scalia, 2012). Later, Reinitzer, with the guidance from German physicist Otto Lehmann, concluded that his cholesteryl materials were homogeneous but existed in a soft solid-like state, giving rise to the term “liquid crystal”. In 1922, G. Friedel’s prestigious work in classifying the types of LCs, introducing the terms such as “mesophases”, “mesomorphic” and “mesogen” and emphasising the importance of the optical microscope as the accurate scientific tool for LC studies has helped gained attention from the scientists.

The second phase, from 1925 to 1959, was characterized by ongoing debate and discussion within the scientific community, with notable contributions from scientists such as Fréedericksz, Zolina, Zocher, Ostwald, Lawrence, Bernal and Sir W. H. Bragg. Although the two world wars had heavily impacted, significant progress was made in understanding the structure-property relationships of LCs and the development of appropriate scientific instruments to study LCs.

Starting from 1960 onwards, the LC science expanded rapidly and globally. This era also saw the commercialization of the first twisted nematic liquid crystal displays (LCD), which catalyzed the demand for more complex LC devices. The period between 1980 and 2000 witnessed the introduction of the first full-colour LCDs, marking a significant milestone in the technological applications of LCs.

In 2007, Pal et al. and Yoshizawa et al. each pioneered novel research topics within the field of LC science, focusing on the S-S bridged dimers and S-shaped dimers, respectively. Following these foundational studies, several research groups such as Kundu et al., (2009), Lee et al., (2012), Osman et al., (2014), Tufaha et al., (2023) and Yeap et al., (2014) further explored the properties on the S-shaped S-S bridged dimers. The dimers reported are relatively shorter, featuring with only one single flexible spacer on each peripheral side and often attached with terminal halogen or polarizable groups. Despite these contributions, it is disheartening to note the slow progress in advancing the field of S-shaped S-S bridged dimers and oligomers over the past 17 years.

The exploration of the mesomorphic phases has never been in a halt since the discovery of LCs in the 19th century. Researchers are consistently uncovering novel types of liquid crystalline phases and developing innovative approaches to maximize their unique properties. This ongoing research not only deepens our understanding of these fascinating soft condensed materials but also paves the way for new technologies and applications across various fields.

## **2.2 Classes of liquid crystals**

LCs exist in two main classes, which are the thermotropic and lyotropic LCs (Lagerwall & Scalia, 2012).

### **2.2.1 Thermotropic liquid crystals**

For the term ‘thermotropic’, temperature is the dominant control parameter in influencing the mesomorphic phase without solvent. Mesomorphic behaviour can be obtained by either melting the solid or cooling the isotropic liquid. Thermotropic LCs can be composed of rod-like (calamitic) or disc-like (discotic) molecules, having the core system constituted from a combination of aromatic rings and flexible terminal

chains, generally the aliphatic hydrocarbons (Lagerwall & Scalia, 2012; Ong & Ha, 2013).

### **2.2.2 Lyotropic liquid crystals**

Lyotropic LCs only form the mesophase in the presence of suitable solvent, most often water, coupled with thermal change and concentration when necessary. In lyotropic phase, the crystalline order is broken down and the building block is often made up of molecules which organized into micellar structure. The formation of micelles is due to the amphiphilic property of anionic, cationic and non-ionic shown by the constituted molecules. Amphiphiles which are made up of hydrophilic and hydrophobic parts have similar morphology and properties to the biological materials. For instance, the cell membranes in our body are built up from the mesogenic amphiphilic lipids (Bouligand, 1998; Lagerwall & Scalia, 2012). It is also found that LCs that possess defects and textures can transform into different shapes in tissues and organs to provide biological functionalities, which open up a new research field in biological morphogenesis. Besides that, lyotropic LCs have been actively studied in industries such as oil, food and detergent as their texture and viscosity could be controlled by specific measures. In the lyotropic phase, the amphiphiles can arrange themselves through self-assembling into different arrangements at different amphiphile concentration. Examples of lyotropic phases are the lamellar phase, hexagonal columnar phase, reverse hexagonal columnar phase, micellar cubic phase, bicontinuous cubic phase and inverse micellar phase (Ghamsari & Carlescu, 2021).

### **2.3 Liquid crystal phases**

The common LC phases reported are the nematic phase, smectic phase, chiral smectic phase, lamellar phase, columnar phase, twist-bend nematic phase, cholesteric

phase, blue phase, twist grain boundary phase, cubic phase and banana phase. These mesophases can exhibit either in a monotropic, enantiotropic or polymorphic behaviour.

The nematic (N) phase is the simplest mesophase and it will be further elaborated in section 2.4.1. When one-dimensional positional order is added into the simplest N phase, the molecules are arranged randomly into layers along one specific direction and smectic (Sm) phase for thermotropic LCs or lamellar phase for lyotropic LCs is obtained (Lagerwall & Scalia, 2012). SmD phase is now known as cubic phase and is very common for lyotropic LCs (Binnemans, 2005; Gray, 1998). Interestingly, the addition of bent conformation can make the Sm phase to be chiral (Sm\*). When a stronger degree of bending is added, the bent molecules will then exhibit banana (Bn) phase (Lutfor et al., 2009). When chirality is added into the nematogens, cholesteric phase which has the molecules assembled in a helical manner can be exhibited (Ghamsari & Carlescu, 2021; Khoo, 2022).

In columnar (Col) phase, the building units are oriented on a two-dimensional lattice with long range positional order along two directions (Lagerwall & Scalia, 2012). In thermotropic LCs, the columnar order is structured by the discotic mesogenic units such as disc- or plate-like molecules stacking up as in piles of coins which respectively are placed hexagonally on the lattice points. In lyotropic LCs, the columnar order is shaped by infinite long rod-like micelles positioned perpendicular to each rod on a two-dimensional lattice.

Twist-bend nematic ( $N_{TB}$ ) phase is reported to be exhibited mostly by the LC dimers with equivalent mesogens or bimesogens and higher oligomers. The formation is possible when the local director experiences the periodic deformations such as twist and bend, forming a conical helix tilted in respect of the helical axis.  $N_{TB}$  phase is rather

interesting as spontaneous chirality can be observed regardless the chirality of the molecules (Paterson et al., 2017).

When the twist in the orientational order occurs in at least two directions in the plane perpendicular to the molecular long axis, a double twist cylinder is obtained (Davis & Goodby, 2014). However, the intersection between these double twists is unable to occupy the entire space in the three dimensional. Hence, these cubic arrays of defects form the blue (BP) phase. The BP phases are usually observed in between the isotropic and  $N^*$  phases within an extremely narrow temperature range (Kikuchi, 2008). The twist grain boundary (TGB) phase is only observed in chiral molecules and is found as the intermediary phase when liquid or  $N^*$  phases change to Sm phase such as  $N^*$  to  $SmA^*$  or liquid to  $SmC^*$  and gives rise to corresponding  $TGBA^*$  and  $TGBC^*$  phases, respectively. In the  $TGBA^*$  phase, the helical structure of  $N^*$  collapses into the layered  $SmA^*$  structure, creating a balance issue. Screw dislocations form to allow both structures to coexist and create grain boundaries (Davis & Goodby, 2014).

### 2.3.1 Nematic phase

Nematic phase, usually with the acronym of N phase, is the simplest liquid crystalline phase. It has the least ordered phase and is considered as one-dimensional order exhibited by the rod-like (calamitic) molecules, with exhibition of long-range orientational without long-range positional order (Binnemans, 2005; Lagerwall & Scalia, 2012). In Figure 2.1 (a), the long molecular axes usually align parallelly to a principal symmetry axis which is commonly named as the director  $\mathbf{n}$ . In ordinary N phase, the full rotational symmetry around the  $\mathbf{n}$  makes the phases uniaxial and consisting two independent components such as the permittivity tensors which show the directions parallel ( $\epsilon_{||}$ ) and perpendicular ( $\epsilon_{\perp}$ ) to  $\mathbf{n}$ . Permittivity is an indicator showing the effect of dielectric medium on the material and how it is influenced by the

electric field (Ghamsari & Carlescu, 2021). In Figure 2.1 (b), the rotational symmetry of the non-chiral N phase is  $D_{\infty h}$  in which the infinite-fold rotation axis is along the director  $\mathbf{n}$  and a vertical mirror plane as well as an infinite number of twofold rotation axes are perpendicular to  $\mathbf{n}$  (Lagerwall & Giesselmann, 2006). N phase is non-polar because the polar vector is forbidden in any direction as the symmetry is too high. Most of the LCs exhibit a uniaxial N phase because their director  $\mathbf{n}$  can be oriented by the external magnetic or electric field. However, LCs that exhibit biaxial N phase are more popular due to their higher sensitivity to external stimuli than the uniaxial N phase. The uniaxial N phase is usually found to be exhibited by the calamitic or discotic mesogenic units whereas the biaxial N phase is found in bent-core mesogenic units. N phase has low viscosity which makes it easily deformed through splay, twist and bend by small external forces (Figure 2.2). Hence, LC molecules move freely in N phase with three translational degrees of freedom while maintaining their long-range directional order (Ghamsari & Carlescu, 2021).

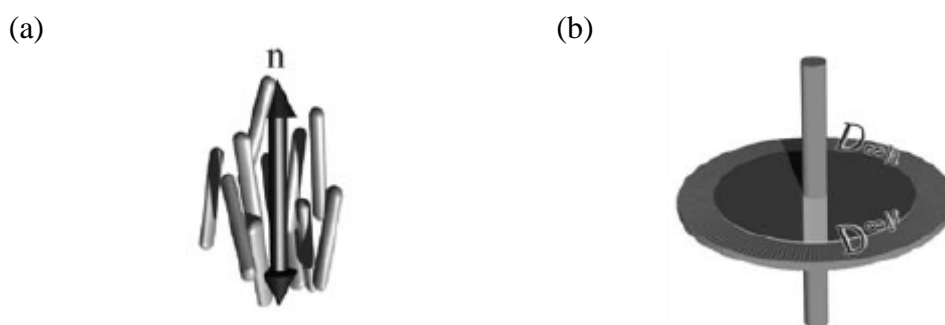


Figure 2.1 (a) Molecular organization and (b) symmetry (right) of the N phase. The rotational symmetry axis corresponds to the centre column of the molecular system. Rods and spiral imply the imaginary chirality of the molecule. The vertical symmetry indicates the axis of highest symmetry. The continuous ring of twofold axes represented the infinite number of twofold axes in the mirror plane of  $D_{\infty h}$  (Lagerwall & Giesselmann, 2006).

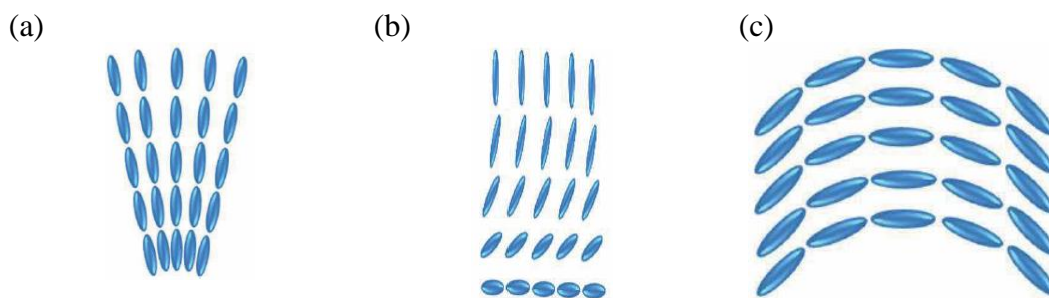


Figure 2.2 (a) Splay, (b) twist and (c) bend deformations (Ghamsari & Carlescu, 2021).

## 2.4 Non-linear disulphide centred liquid crystals

As mentioned in section 1.2, the linear form of LC oligomers is divided into the dimer, trimer, tetramer and so on, depending on the number of mesogenic units linked through the flexible spacers. When one or more mesogens is connected at the lateral position of a molecular structure, the non-linear molecular forms such as dendrimers (Aya et al., 2021), U-shaped (Rahman, Sarkar, et al., 2015), Y-shaped (Yoshizawa et al., 2006),  $\lambda$ -shaped (Yamaguchi et al., 2005), H-shaped (Sayama et al., 2019), S-shaped (Osman et al., 2016), V-shaped (Salwadi et al., 2023) and butterfly-shaped (Park et al., 2015) will be formed. The non-linear LCs are reported to exhibit different liquid crystalline behaviours, physical properties and high ordered structures (Osman et al., 2017b; Osman et al., 2016). The non-linear forms have unlocked a myriad of possibilities in the design of molecular structures, giving rise to novel and previously unidentified mesophases, in stark contrast to the more predictable behaviour of linear LC oligomers. For example, the review by Ting et al. (2020) has mentioned examples of new mesomorphic properties found in the non-linear LC oligomers with minor structural difference such as bent-core nematics with cybotatic clusters,  $\text{SmC}_x$ , chiral crystal phase,  $\text{SmX}_1$  and  $\text{SmX}_2$ . It is difficult to report more on the non-linear S-shaped disulphide centred LC oligomers as this topic is underexplored and little documented. In addition, most of the reported non-linear S-shaped LC oligomers were centred with

biphenyl and alkyl groups but rarely reported for those with S-S center (Cruickshank et al., 2023; Ogasawara et al., 2008; Osman et al., 2017a; Osman et al., 2017b; Osman et al., 2016; Yeap et al., 2017).

The first series of S-shaped LC oligomers equipped with central biphenyl group was revealed by Yoshizawa et al. (2007) in which he described that the S-shaped oligomer was actually formed from two U-shaped systems connected through flexible linker. It was found that more frustrated or uncommon phases were likely to be induced when the flexible linking spacers were lengthening and the intramolecular interaction between the mesogenic units affected the structural packing, supported by a recent documentation by Cruickshank et al. (2023). They also discovered the exhibition of a novel unidentified biaxial smectic phase when non-linear even-membered S-shaped LCs were mixed with phenylpyrimidine derivatives as a binary mixture, suggesting the potential of non-linear oligomers in a binary mixture to induce unexplored phase. The pronounced odd-even effect was found in the phase transition temperatures due to the different spacer parity. In the work reported by Osman et al. (2016), the series of S-shaped oligomers exhibited monotropic phase for the even parity and enantiotropic phase for the odd parity. It is reported that the elongation of outer alkyl spacer loosened the molecular rigidity and hence reduce the smectic stability. It is known that the even-membered oligomers have sufficient synergy between the conformational and orientational orders to drive the interconversion of the linear and bent forms but there is a large energy gap between the conformational and orientational orders for the odd-membered oligomers. This difference can be applied to the odd-even effect and smaller entropy change observed for the S-shaped oligomers. In work by Cruickshank et al. (2023), they also revealed that the transition temperatures increased when the alkyl spacer length increased and became easier to be packed efficiently into the alignment.

Pal et al. (2007) reported the first series of linear S-S centred dimers and shown how the geometry and torsion energy of the S-S group affected the molecular shape and the transition temperatures when there was no steric hindrance possessed on the group through the computational calculation. S-S linkage is rather unique than other common linkage groups because it does not have attached projecting bonds, making it relatively unhindered due to the low rotational barrier about the linkage (Kundu et al., 2009). Thus it has been claiming that the unique property promotes the polymorphism behaviour and odd-even effect (Lee et al., 2012; Osman et al., 2014; Tufaha et al., 2023). It was also reported that enantiotropic property and higher ordered molecular alignment were tend to be exhibited from these S-S bonded LC oligomers when the alkyl spacer was lengthening. A recent report from Tufaha et al. (2023) showed the bent C-S-S-C torsion angle was an important prerequisite for the exhibition of twist-bend nematic phase from non-linear S-S centred dimers especially the one with odd-numbered spacer. This statement is consistently proved by recent works by Arakawa, Ishida, et al. (2021), Yu and Wilson (2022) and Majewska et al. (2022). The odd-membered dimers have higher potential to exhibit the uncommon twist-bend nematic phase as the bent shape facilitates better molecular interactions between the mesogenic units with the additional polar order in the phase (Arakawa, Ishida, et al., 2021; Arakawa, Komatsu, et al., 2021). The unique twist-bend nematic phase is considered one of the significant discoveries in recent LC science and these bent mesogens have been a popular component in various applications such as the photo switchable optical devices and photoalignment technologies. On varying the number of methylene units in the spacer, odd-even effect was observed in the transition temperatures and entropy change as a result of the change in the spacer parity. They also mentioned that the even-membered dimer has linear conformation which made it to be more compatible with the nematic environment than

the odd-membered dimer which is more bent to understand the transition behaviours observed (Cruickshank et al., 2023; Kundu et al., 2010). In addition, investigation on the introduction of only one sulphur atom into the alkyl spacer as the centre was conducted and found less pronounced molecular structural difference and transitional properties due to the smaller C-S-C bond angle and increased dipolar interactions.

## 2.5 Factors affecting mesomorphic behavior

Since the discovery of the mesophases, researchers have conducted studies on the effect of spacer length and parity, terminal chain length, the presence of odd-even effect, the presence of substituent at a strategic location along the central core, the presence of halogen in either terminal or lateral position, conventional and unconventional molecular shapes in exploring more unknown potentials of the LC science.

### 2.5.1 Linking groups

Common linking groups such as the alkyl spacers  $(\text{CH}_2)_n$ ,  $\text{HC}=\text{CH}$ ,  $\text{H}_2\text{CO}$ ,  $\text{O}=\text{C}-\text{O}$ ,  $\text{COS}$ ,  $\text{N}=\text{N}$  and  $\text{HC}=\text{N}$  have the property of producing bent molecular shape and hence affect the mesogeneity of the constituted molecule. Not only that, the linking groups have other effects such as the conjugative interaction with the aromatic groups, polarity, *trans/cis* isomerization which affect the mesomorphic behaviours as well as affecting the transitional temperatures and properties (Demus, 1998). For example, linking groups with double bonds have lower  $T_c$  compared to those with triple bonds. When a benzene ring is connected to  $-\text{OCH}_2$  in a molecule, there is an increase in the hindrance of bond rotation between the oxygen atom and the aromatic hydrocarbons. Hence, the nematogeneity is higher than in the case of a benzene ring connected to  $-\text{CH}_2\text{O}$  in a molecule. The high aromaticity of the linking group can have high

mesogenic potential and  $T_c$  compared with those with single bond. When there is a presence of strong polar groups such as CN and NO<sub>2</sub> in a compound, these groups can increase the molecular length (almost a factor of 2) and breadth (factor of 1.1-1.4) by dimerization. Thus, they have higher density due to the packing fraction and lead to higher  $T_c$ . It is also reported that linking group such as O=C-O which is next to the aromatic ring favours the lamellar packing and hence induces the Sm phase instead of the N phase due to the conjugative interaction (Lim et al., 2017). Popular linking groups such as N=N and HC=N can alter the molecular linearity and molecular stiffness since the double bond restricts the freedom of rotation. As a result, molecular anisotropy increases and leads to the formation of mesomorphic behaviour from the compound. It is known that the HC=N unit is more polar than the N=N unit because N=N has a zero dipole moment. Researchers support that the dipole moment plays a role in the exhibition of the Sm phase and its thermal stability as a higher dipole moment enhances molecular polarizability and intermolecular cohesive forces (Yeap et al., 2012).

### **2.5.1(a) Azobenzene**

Azobenzene or simply azo (N=N) group, is a very useful element in the synthesis of LCs either attached to the molecular structure through chemical reactions or as a dopant in the LC host (Alshargabi et al., 2013; Hegde et al., 2015). They have high thermal stability, high stimuli-responsiveness and favour the exhibition of mesomorphic behaviour. The introduction of the rod-shaped N=N group into the mesomorphic system can increase the mesomorphic stability, molecular length and molecular polarizability (Nakum et al., 2022). Furthermore, it also possesses photosensitive ability, unique reversible photo-switchable property of *trans-cis* induced by light, dimerization in cross linking material and irreversible photodegradation (Madihlagan et al., 2019; Ooi et al., 2014; Rahman, Biswas, et al., 2015; Sun et al.,

2024). These attractive features made the azo group superior to other linking groups such as azomethine and ester (X. Wang et al., 2020). Upon the UV irradiation at 365.00 nm, the stable *trans*-isomer will isomerize to *cis*-isomer. While for the reconversion from *cis*- to *trans*-configuration, it can be done by keeping the unstable *cis*-sample in the dark or irradiate the sample with white light at 450.00 nm. The process of keeping the sample in the dark for the *cis*-to-*trans* conversion is known as thermal back relaxation (Nakum et al., 2022; Osman et al., 2017a; Sun et al., 2024). The duration of thermal back relaxation exhibited from a LC can help to determine its potential to be used in related applications such as photonic computing, optical imaging system, dynamic holography and pattern recognition (Yeap, Abdul Rahim, et al., 2016). For instance, LC containing N=N with long duration of thermal back relaxation can be used for the creation of optical storage devices whereas the one with a fast or short duration of thermal back relaxation can be used in applications such as molecular switches (Babamale et al., 2024; Hegde et al., 2015).

#### **2.5.1(b) Schiff base**

The Schiff base is a compound containing the azomethine unit (HC=N). The HC=N unit is one of the well-known linking groups used to connect two core groups in a molecule. Schiff base is formed easily from the reflux between a primary amine and an aldehyde. HC=N in the molecular structure not only helps to maintain the molecular linearity, it is also reported to favour the exhibition of mesomorphic behaviours over a broad temperature range (Jevtovic et al., 2023; Ong & Ha, 2013). It is reported that the presence of HC=N increases the molecular length, molecular polarizability and the mesomorphic stability of the mesogenic system as well (Ahmed et al., 2020; Nakum et al., 2022). Besides that, LC oligomers consisting of HC=N are reported to be used in the chemical, biological, optical, medicinal and material applications such as stabilizer,

biological activity agent and chelator (Salwadi et al., 2023). Similar to N=N, the photochromic HC=N has the ability to undergo light-induced *trans-cis-trans* isomerization as well (Alnoman et al., 2020; Omar et al., 2023; Zakaria et al., 2021). In the isomerization property, long and short duration of thermal back relaxation shown by the LC containing HC=N also exhibit considerable promise and significant applications such as optical storage devices and molecular switches (Jevtovic et al., 2023).

### **2.5.2 Flexible alkyl spacer**

It is well known that dimeric LCs depend heavily on the length and parity of the spacer within the molecule (Yeap, Osman, et al., 2016). The flexible spacer in a molecule plays an important role in contributing to the molecular anisotropy and the relative orientation of the mesogen. It is reported that the LCs with even-membered spacer have a linear or antiparallel conformation whereas LCs with odd-membered spacer have a bent or inclined conformation. The different conformations of the LCs will exhibit different transitional properties (Imrie & Luckhurst, 1998). For example, the dimeric LCs show odd-even effect in the phase transition temperatures in such that the odd-membered dimer has lower  $T_m$  than that of the even-membered dimer. It was also reported that the increment in terminal spacer length favoured the N behaviour due to the reduction in the positional order (Mohammad et al., 2016). In addition, Iskandar et al. (2020) also revealed the lengthening terminal alkyl chain reduced the thermal stability of the LC dimer. It is also found that the attachment of odd-numbered carbon atom causes higher length-to-breadth (L/D) ratio than the even-numbered carbon atom does (Demus, 1998). This is why we often found the odd-even effect on the mesomorphic behaviours.

### 2.5.3 Substituent

The alkyl, alkyloxy, halogen, nitro and cyano groups are the common terminal and lateral substituents. The types and sizes of the terminal groups help in increasing the molecular polarizability and affect the mesomorphic property. For example, Yeap et al. (2014) and Iskandar, Yeap, Yusop, et al. (2024) reported the highly polarizable and large sized substituent in the terminal group increased the stability of mesophase more than other types of substituents. Yeap et al. (2013) also reported the influence of the polarizability of the halogen on  $T_c$  in such that the large sized I atom exhibited higher  $T_c$  than Cl, Br and alkyl group and thus suppressed the mesomorphic behaviour. Lim et al. (2017) reported that the longer terminal alkoxy chain have stronger *Van der Waals* interactions and more possible intertwining between the alkoxy chains, favouring the lamellar packing. As a result, the presence of terminal alkoxy chain in LCs has been well reported in aiding the exhibition of enantiotropic Sm phase (Ismail et al., 2023). Salwadi et al. (2023) and Iskandar, Yeap, Maeta, et al. (2024) also reported that a longer terminal alkoxy chain favours lower transition temperature of N-I as the lengthening terminal alkoxy chain will have increased molecular flexibility and weaker molecular packing interaction.

In general, the lateral substituent is reported to have reduced the  $T_m$  and  $T_c$  because their presence broadens the molecular structure by increasing the breadth of the molecule (Ahmed et al., 2020; Imrie & Luckhurst, 1998; Jevtovic et al., 2023). Dave et al. (2012) extensively investigated the different types of lateral substituent on various positions in the mesogenic system and reported that the LCs with lateral substituent had shorter mesophase range than the one without lateral substituent. At the same time, flexible lateral alkoxy or alkyl substituent are interesting as well. Their effect on reducing  $T_m$  and  $T_c$  diminishes upon the increment of the chain length. Reports showed

the smaller sized lateral substituents have less depression effect on the  $T_c$  than the larger ones without much considering on the polarity (Bahadur, 1990; Gray, 1976). Sometimes, lateral substituents such as -OH group may also increase the shielding effects due to the intramolecular hydrogen bonding which increase the molecular stiffness and hence higher  $T_m$  and  $T_c$ . Not only in dimers and higher ordered oligomers, but a study by Xie et al. (2016) reported that the series of LC monomers with lateral reactive group had their  $T_m$  decreasing upon the increase in length of the lateral substituent.

When there is an elongation of the lateral chain, the aspect ratio of the LC might as well increase and thus the LC has a lower thermal stability. In the case of having molecules that are large enough, the  $T_m$  and  $T_c$  are predicted to be high. When the lateral substituent in a compound is long and large with rings, it is assumed that the lateral chain is positioned nearly parallelly to the constituted molecule and considered a variant of the rod-like molecule. When a compound with bulky lateral substituent, the mesogenity and mesomorphic behaviour cannot be predicted well and it is not easy to understand if there is mesophase appears.

## **2.6 Applications of liquid crystals**

Since the discovery of LCs in 1888, it has been triggering and engaging the scientists around the world to indulge in the exploration of LCs for almost eight decades until they came up with the idea of utilising the simplest mesophase, which is the N phase in display applications (Lagerwall & Scalia, 2012). Besides making progress in the purely LC field, the LCs have been highly considered in other fields of soft matter science such as the polymers, colloids, nanotechnology and biotechnology. The extraordinary balance between molecular order and fluidity and high sensitivity towards stimulus has brought the LCs towards a broad range of possibilities in development of applications (Wang et al., 2021).

The rapid development in the electronic display design and construction has led to the launching of digital devices such as smart devices, electronic devices and calculators (Ghamsari & Carlescu, 2021; Iwan et al., 2009). In the display application, three main types of LCD which are the transmissive, reflective and trans-reflective LCDs have been developed and widely used. The LCs are capable of being flat paneled, showing high brightness and resolution, saving energy, low weight and having a customizable outlook that can fit the industrial demand. For instance, the ferroelectric LCs are mainly used in the fast high-resolution microdisplays such as the view-finders for digital cameras and camcorders (Lagerwall & Giesselmann, 2006).

LCs are also being used in the non-display applications such as light modulator, optical interconnects, optical correlators, switches, LC grating and dimming glass (Crossland & Wilkinson, 1998; Qian et al., 2023). Due to their unique property, LCs can also act as the anisotropic solvents for spectroscopic, chemical reaction and gas chromatographic applications (Leigh & Workentin, 1998). In addition, the LCs have high sensitivity towards the electric and magnetic fields. Hence, they outperform the solid alternatives as they are easier to be aligned over large area and suitable for solution processing such as the LC emulsion. Particularly, LCs have been used for designing and building organic systems and transistors by self-assembly for long time (Sergeyev et al., 2007). LCs are also widely used in the sensor application such as the temperature sensors, biosensors and disposable thermometers (Algorri et al., 2014; L. Wang et al., 2020). LCs such as LC elastomers which have high sensitivity towards heat, light, humidity and magnetic field are great components to be used in the soft robotic applications. With minimal stimuli, the LCs can perform different locomotion such as walking, climbing, crawling, rolling, creeping and jumping to fulfill the application demand in different environments (Xiao et al., 2020).